13

Automated Individual Tree-Crown Delineation and Treetop Detection with Very-High-Resolution Aerial Imagery

Le Wang and Chunyuan Diao

CONTENTS

13.1 Introduction 223
13.2 Study Sites and Data Preparation 225
13.2.1 Study Sites 225
13.2.2 Data Preparation 225
13.3 Methods 226
13.3.1 Enhance Tree-Crown Boundaries 226
13.3.1.1 Dyadic Wavelet Decomposition 226
13.3.1.2 Edge Probability with the Magnitude Information 227
13.3.1.3 Scale and Geometric Consistency Constraints 228
13.3.2 Edge Detection 228
13.3.3 Treetop Identification 229
13.3.3.1 Treetop Detection Based on Radiometric Characteristics 230
13.3.3.2 Treetop Detection Based on Spatial Characteristics 230
13.3.3.3 Marker Image Generation 231
13.3.4 Marker-Controlled Watershed Segmentation 231
13.4 Results 232
13.5 Discussion 235
13.6 Conclusion 235
References 236

13.1 Introduction

Forest stands, as the basic units in forest management, play a pivotal role in understanding the function and service of the forest system. A stand is a contiguous area that contains a number of trees that are relatively homogeneous or similar in species composition or age and different from adjacent areas (Lindenmayer and Franklin 2002). Several parameters of the stand are of particular interest to foresters, including tree density, stand basal area, stand diameter, stand height, crown closure, stand volume, stand table, and site index. Traditionally, to acquire those parameters, field plots with a random, stratified, or systematical sampling scheme have to be designed and measured, which is usually expensive and labor-intensive. Nevertheless, timely and accurately obtaining the stand information is critically important for updating the forest inventory (Spurr 1948) and for conducting

ecological studies with those parameters as the input (Palace et al. 2007). As remote sensing imagery is more readily accessible, information gathering becomes more frequent and cost-effective.

In the 1940s, visual interpretation of medium- and large-scale aerial imagery for forestry emerged (Brandtberg 1999). However, the manual interpretation method is usually time-consuming, labor-intensive, and biased by the interpreter's experience, which to a great extent triggered the development of automated or semiautomated methods for individual tree recognition. With the increasing availability of very-high-resolution (VHR: meter or submeter level) imagery, the development of automated computer-based photo interpretation has been spurred (Gong et al. 1999), and various algorithms have been developed for automatically delineating individual trees, which basically falls into four major types: local maximum (LM)-based methods (Blazquez 1989; Dralle and Rudemo 1996), contour-based (CB) methods (Gougeon 1995; Pinz et al.1993), three-dimensional (3D) model-based methods (Gong et al. 2002; Sheng et al. 2001), and template matching (TM)-based methods (Pollock 1996; Tarp-Johansen 2002).

The LM method attempts to detect the treetops by finding the local maximum of the image with the assumption that the peak of the tree-crown reflectance is located at or very close to the treetop (Brandtberg and Walter 1998). Despite being fast and simple, it performs poorly as image illumination conditions vary. The TM method characterizes the tree morphology at different locations of the image by considering the trees' geometric and radiometric properties with a series of models. With the information gained, the TM procedure (Pollock 1996) is implemented to search for the locus of best matching trees. In comparison, 3D-based methods have been utilized by fewer researchers. Sheng et al. (2001) applied parametric tree-crown surface model-based image matching to obtain an improved tree-crown surface reconstruction. Gong et al. (2002) developed an interactive tree interpreter for the semiautomatic tree-crown segmentation as an improvement. This method, however, has to determine the treetop locations separately on the left and right epipolar images to be fully automated. The CB method searches for the delimiter between tree crowns and their background by following the intensity valleys underlying the image (Gougeon 1995) or by detecting the crown boundary with edge-detection methods (Brandtberg and Walter 1998). Edge-detection methods are seldom applied in tree-crown delineation mainly because of two difficulties. On the one hand, intensity changes vary with the scale. At the finer scale, tree branches are the major components accounting for the changes in intensity, whereas at the increasing coarser scale, tree internal structures are gradually suppressed and a tree crown tends to merge with its neighbor (Brandtberg and Walter 1998). In that sense, the clusters of trees are where the changes occur. Hence, finding the appropriate scale for delimiting the individual tree-crown boundary is difficult. Considering that tree crowns tend to have different sizes within the forest stand, it is impossible to choose a scale applicable for all the individual trees. Accordingly, information on multiple scales should be investigated and integrated in order to more accurately delineate the individual tree crown. On the other hand, the edge-detection method can only create raw primal sketches as a low-level image processing method. Incorporating the expert knowledge or biological knowledge about the tree-crown shapes into high-level individual tree-crown delineation is inevitably crucial for producing a more accurate result.

To bridge the gap between edge detection and tree-crown delineation, three objectives are set in this study: (1) to incorporate the multiscale scheme for enhancing tree-crown boundaries while suppressing excessive texture inside; (2) to locate treetops with consideration of both geometry and radiometry information; (3) to develop a more advanced

two-stage tree-crown detection method, namely edge detection followed by marker controlled watershed segmentation. Hopefully, with the multiscale preprocessing method and the two-stage approach, treetops can be more accurately located and tree-crown boundaries can be more efficiently delineated.

13.2 Study Sites and Data Preparation

13.2.1 Study Sites

The study area is a young ponderosa pine forest stand located at 38°53′42.9″N, 120°37′57.9″W, adjacent to Blodgett Forest Research Station, a research forest of the University of California, Berkeley. The stand has the following characteristics: an average diameter of 9.81 cm at breast height (DBH), a density of 420 stems/hectare, and an average height of 4.05 m. In 2000, a precommercial thinning took place and most of the shrubs and grass were cut down. The dominant species thereafter in the stand was almost the 10- to 11-year-old ponderosa pine (*Pinus ponderosa*).

13.2.2 Data Preparation

A 1:8000 aerial photograph was acquired by an aerial camera with a focal length of 152.9 mm in May 2000, under the uniform cloud cover condition. Then it was scanned at 1000 dpi, with a 20.3 cm spatial resolution digital image produced. A subset image with the size of 500 × 500 pixels was chosen in this study, approximately a ground area of 10,404 m^2 (Figure 13.1). A total of 58 trees, identified both on the ground and on the aerial image, were selected in the subset image. For each tree, the crown diameter was

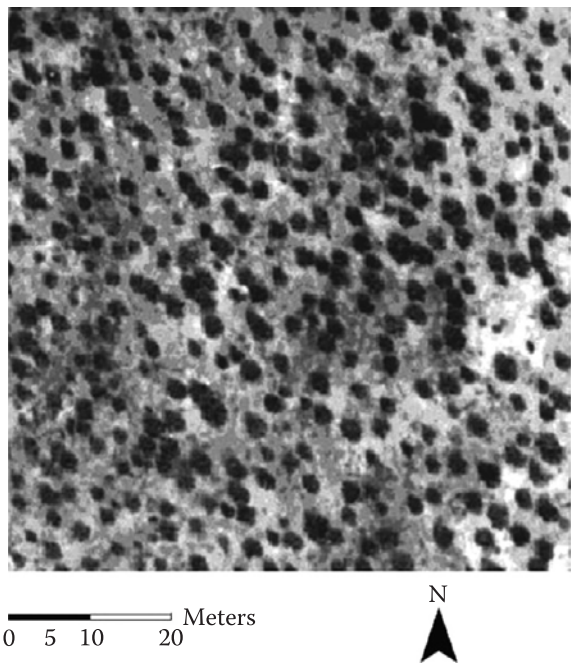

FIGURE 13.1
The scanned aerial photograph in our study area.

measured on the ground in two directions: one along the maximum axis and the other along the perpendicular direction. As reference data, the radius of the tree crown can then be calculated by averaging the two measurements. More details of the data can be found in Wang (2010).

13.3 Methods

The tree-crown delineation algorithm can be divided into three stages. The first stage applies the scale-space theory to preprocess the image in the multiscale scheme for enhancing the true tree-crown boundaries (Wang 2010). The second step utilizes an edge-detection method to obtain primal tree-crown boundaries (Wang et al. 2004). The third stage can be separated into two main parts: treetop marker selection and marker-controlled watershed segmentation (Wang et al. 2004). The following sections describe each step in detail. Further information can be found in Wang et al. (2004) and Wang (2010).

13.3.1 Enhance Tree-Crown Boundaries

To produce accurate crown delineation, the tree-crown information should be investigated at multiple scales. Wavelet-based methods (Mallat 1989) based on scale-space theory can be applied to decompose the original information with multiresolution approximation. By exploring the evolution of the edges, the true tree-crown boundaries can be distinguished from edges that correspond to the tree branches and twigs, and thus, textures of the true tree can be strengthened, while those within a single tree will be suppressed.

13.3.1.1 Dyadic Wavelet Decomposition

Scale-space theory aims at making significant structures and scales explicit (Lindeberg 1993). The idea is to link low-level features detected at different scales in scale space, thus facilitating the identification of high-level objects (Lu and Jain 1992). By convolving the original image with the transformed and dilated wavelet, the original image can be decomposed as one approximation image together with various difference images at different scales. The advantages of the wavelet decomposition include no correlation among images of different scales and the acquisition of local edges' information with coefficients of the wavelet orthonormal basis expansion.

In this study, the cubic spline function mentioned in Mallat (1989) was adopted as the scaling function or as a low-pass smoothing filter. The wavelet function can be considered as the derivative of the smoothing function with orthonormal characteristics. Since calculating the wavelet coefficients at every possible scale is impractical, the dyadic wavelet decomposition with only scales of the power of 2 was used. At each decomposed level, four wavelet coefficients, namely approximate, horizontal, vertical, and diagonal coefficients, can be obtained, and then the gradient magnitude (Equation 13.1) and orientation (Equation 13.2) can be calculated with the purpose of quantifying the evolution of edge pixels from different sources, that is, tree crown or branches, across the scale space.

$$M_{\text{edge}} = \sqrt{\left(W_{2^j}^{\text{h}}\right)^2 + \left(W_{2^j}^{\text{v}}\right)^2} \tag{13.1}$$

$$A_{\text{edge}} = \arctan\left(\frac{W_{2^j}^{\text{v}}}{W_{2^j}^{\text{h}}}\right) \tag{13.2}$$

where M_{edge} denotes the gradient magnitude and A_{edge} is the gradient orientation. $W_{2^j}^{\text{h}}$ and $W_{2^j}^{\text{v}}$ stand for the horizontal and vertical coefficients, respectively, in the wavelet decomposition at the scale 2^j.

13.3.1.2 Edge Probability with the Magnitude Information

With the wavelet decomposition coefficients, the gradient magnitude can be obtained at each scale and the threshold can be set for separating the edge pixels from the background. However, using a single threshold to judge the edge pixel is apparently inappropriate or inefficient on a complex forest image. Edge probability, from another perspective, provides more information than the single threshold method and can distinguish the edge pixel more accurately.

Scharcanski et al. (2002) modeled the gradient magnitude of background-related pixels with a Rayleigh probability density function (Equation 13.3). Similarly, the magnitude of edge-related pixels can also be modeled by the Rayleigh probability density function with the variance of edge pixels (Equation 13.4). With those two probabilities, the overall probability of a pixel being the gradient magnitude of r is shown in Equation 13.5.

$$P_j(r/\text{background}) = \frac{r}{\left[\sigma_{\text{background}}^j\right]^2}\exp^{-r^2}/2\left[\sigma_{\text{background}}^j\right]^2 \tag{13.3}$$

$$P_j(r/\text{edge}) = \frac{r}{\left[\sigma_{\text{edge}}^j\right]^2}\exp^{-r^2}/2\left[\sigma_{\text{edge}}^j\right]^2 \tag{13.4}$$

$$P_j(r) = w_{\text{background}}^j P_j(r/\text{background}) + (1 - w_{\text{background}}^j)P_j(r/\text{edge}) \tag{13.5}$$

where $P_j(r/\text{background})$ is the probability of a pixel having gradient magnitude equal to r, given that it belongs to a background pixel at the scale of 2^j, and $\sigma_{\text{background}}^j$ is the standard deviation of a background pixel's gradient magnitude at the scale of 2^j. It is also the same for $P_j(r/\text{edge})$ and σ_{edge}^j. $w_{\text{background}}^j$ is the prior probability of a pixel being background or noise.

To calculate $P_j(r)$, three parameters, $\sigma_{\text{background}}^j$, σ_{edge}^j, and $w_{\text{background}}^j$, have to be known first. A typical method for solving the unknown parameters is using the maximum likelihood function (Equation 13.6). Then from the Bayes theorem, the probability of a pixel belonging to the edge, given the gradient magnitude being r, can be calculated using Equation 13.7. As a result, the gradient magnitude will be replaced with $p(\text{edge}/r)$ in the following process of enhancing the tree-crown boundaries.

$$[w_{\text{background}}^j, \sigma_{\text{edge}}^j, \sigma_{\text{background}}^j] = \arg\max\left(\prod P_j(r)\right) \tag{13.6}$$

$$p(\text{edge}/r) = \frac{\left(1 - w_{\text{background}}\right)p(r/\text{edge})}{p(r)} \tag{13.7}$$

13.3.1.3 Scale and Geometric Consistency Constraints

Since texture information within the tree crown, that is, branches or twigs, is hard to distinguish from that of true tree crown with the edge probability at a single scale, the evolution of pixels along various scales is checked with the assumption that true-crown boundaries will consistently exhibit a large edge probability, while pixels with undesired texture will only show a large edge probability in a small range of scales. Harmonic mean (Equation 13.8) is chosen in this case to evaluate the scale consistency with the aim of further enhancing the true tree-crown texture and suppressing the undesired ones.

$$P_j(\text{edge}/r) = \frac{M+1}{\frac{1}{P_j(\text{edge}/r)} + \frac{1}{P_{j+1}(\text{edge}/r)} + \cdots + \frac{1}{P_{j+m}(\text{edge}/r)}} \tag{13.8}$$

where $p_j(\text{edge}/r)$ is the edge probability at the scale 2^j, $p_{j+m}(\text{edge}/r)$ is the edge probability at the scale 2^{j+m}, and $M + 1$ is the total number of scales that are included in this analysis.

Besides the scale consistency constraint, tree crowns should also satisfy the condition of geometric consistency, since tree crowns are usually curved in shape and the orientation along the tree-crown boundary should not change significantly. Using Equation 13.2, the gradient direction of each pixel can be assigned and evaluated. A typical example of edge pixels is shown in Figure 13.2 with the gradient direction denoted by an arrow. Thus, the edge probability $p_j(\text{edge}/r)$ can be updated by assigning the weight by the Gaussian function along the gradient direction. The geometric consistency tends to augment the true tree-crown boundary by strengthening the edge pixels with a continuous smooth curve and suppressing the isolated ones. Finally, an inverse wavelet transformation can be used to reconstruct the image with enhanced tree-crown boundary for the subsequent edge detection and tree-crown delineation.

13.3.2 Edge Detection

A forest image is usually composed of tree crown, understory vegetation, and bare soil. Masking out nontree areas and retaining tree-crown objects are inevitably the first step

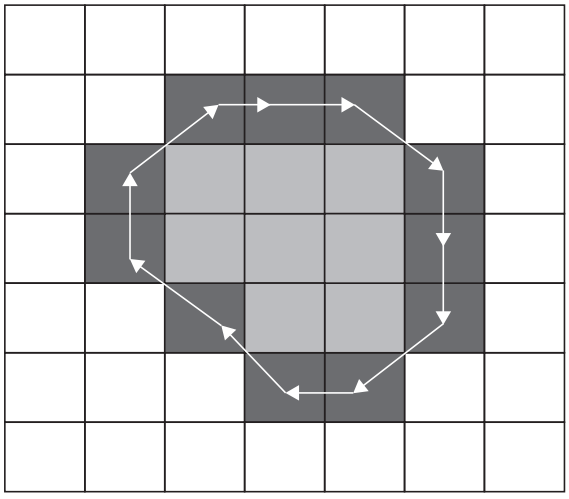

FIGURE 13.2
An example of tree crown's gradient direction of the boundary pixels.

for individual tree-crown recognition. Edge-detection methods, by deriving the initial boundary of the tree crown, can achieve this purpose to a large extent. However, current edge-detection methods can only be applied to a single band. Hence, we applied the intensity–hue–saturation (IHS) transformation to the original aerial-colored image and utilized only the intensity image in the subsequent edge detection.

The Laplacian of the Gaussian (LOG) operator was selected in this study for detecting the edge of the tree crown. The LOG method can be partitioned into two parts. The first part involves a Gaussian smoothing for removing the noise and intensity variation by virtue of a tree's internal structure. For the second part, the pixels corresponding to the zero of the second derivative of the smoothed image were marked as edge pixels, since in an image, an edge indicates the intensity discontinuity and can be captured by the derivative function. The LOG detector can be written as (Marr and Hildreth 1980)

$$\mathrm{LOG}(x,y) = -\frac{1}{\pi\sigma^4}\left[1-\frac{x^2+y^2}{2\sigma^2}\right]\exp\left(-\frac{x^2+y^2}{2\sigma^2}\right) \tag{13.9}$$

The smoothing scale σ in the LOG method implies the minimum width of the edge that can be captured. In our study, the smoothing scale is one pixel, which represents the smallest tree-crown diameter in the image by visual inspection. The LOG operator can also bring about artifacts or phantom edges. To distinguish those phantom edges from the true edges, a method proposed by Clark (1989) was used to remove the phantom edges for the subsequent tree-crown delineation.

With the edge pixels detected by LOG operator, a series of closed contours, indicating the tree-crown boundaries, can be formed with an eight–connectivity scheme. However, those contours obtained may not represent the individual tree crown and typically three scenarios may be included, namely isolated trees, slightly touching trees, or tree clumps (Brandtberg 1999) (Figure 13.3). Isolated single trees tend to form a single circular-shaped contour, while slightly touching trees or tree clumps are more inclined to have irregular or oblong shapes. Hence, further segmentation of those contours is necessary for obtaining the tree-crown boundary on an individual basis. In our study, we identified the treetops within each contour first and then utilized the treetop information as a guide for acquiring the final individual tree-crown boundaries.

13.3.3 Treetop Identification

We treat each closed contour as an object, and for each object, we determine the number of trees it contains by locating the treetops. Treetops can be identified by their unique radiometric and spatial characteristics. With regard to the radiometric intensity, it usually varies in different parts of the tree and reaches the highest on the uppermost

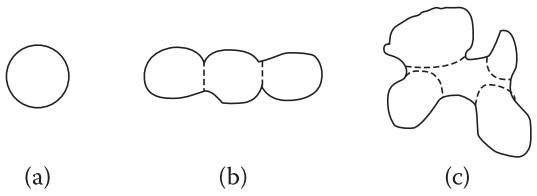

FIGURE 13.3
Three typical cases of objects after edge detection: (a) isolated trees, (b) slightly touching trees, and (c) tree clumps.

sunlit portion of the tree crown. Hence, in our study, a local nonmaximum suppression method was adopted to obtain the treetops in each contour. As regards the spatial characteristic, a treetop is located at or near the center of the tree crown when it is viewed from angles near nadir. Correspondingly, an LM distance method was applied to obtain another set of treetops. The intersection of the two sets of treetops by both methods is identified as the authentic treetop and will be denoted as the marker for the following segmentation.

13.3.3.1 Treetop Detection Based on Radiometric Characteristics

A local nonmaximum suppression method was utilized to detect the pixel with highest radiometric intensity for each crown object as the treetop, based on the gray values of the intensity image from IHS transformation. Specifically, it will use a sliding window to assign a value of one to the center pixel only if all the surrounding pixels' gray values within the window are less than that of the center pixel for locating the treetops (Dralle and Rudemo 1996) and finally create a binary image in which pixels representing the treetops were labeled one and all others were labeled with a value of zero. With respect to the sliding window, the size of the window is vitally important for accurately and efficiently locating the treetop. If the window size is too small, the tree crown with large radius may be assigned more than one treetop. Contrarily, if the window size is too large, trees having smaller crowns may not be detected and assigned a treetop. In our study, a relatively small size of sliding window (3 × 3 window of pixels) was selected with the purpose of not missing the small treetop. For those false treetops assigned by this method, they can be identified and filtered out by the subsequent algorithm in view of treetops' spatial properties.

13.3.3.2 Treetop Detection Based on Spatial Characteristics

Apart from the treetops selected by virtue of the radiometric features, treetops can also be identified from a spatial perspective. An LM transformed distance method can be applied for locating the treetops spatially, with the assumption that treetops are located in the vicinity of the center of the tree crown from the near nadir view. The method can be divided into two parts. First, the geodesic distance between the pixels within each object of closed-contour and the set of exterior pixels was calculated. Then, the regional maximum of the distance image was extracted and labeled as a treetop.

The geodesic distance is a concept borrowed from mathematical morphology by defining the distance between two pixels p and q within the set A as the length of the shortest path connecting p and q in A and defining the distance from any pixel in set A to its complementary set as the path joining that pixel in A with the nearest pixel in the complement of A. To calculate the distance between each interior pixel and the set of exterior pixels, an elementary disk structure element (SE; 3 × 3 window of pixels whose values are equal to 1) was defined by considering the eight-connected neighborhoods of the center location, as opposed to an elementary cross SE with only four-connected neighborhoods. As a consequence, the distance can be measured only along connected paths defined by the SE, and the length of each step is determined by the value of each pixel in the SE. Normally, an SE can represent the geometry of the object to be measured and is usually built as a small window of pixels with values either 0 or 1 (Soille 2003).

With morphologically transformed distance calculated for each interior pixel in the object, a resultant distance image, signifying the distance from that interior pixel to the nearest exterior pixel, can be formed. Accordingly, the regional maximum of the distance image for each object can be extracted. As for the regional maximum, it is defined as a connected group of pixels with a single distance value, and for each pixel in the group, the distance value is greater than or equal to that of the surrounding eight-connectivity neighborhood. As a consequence, the regional maximum is usually located near the center of the object, and thus, those pixels corresponding to the regional maximum are marked as treetops spatially.

13.3.3.3 Marker Image Generation

Two sets of treetops can be formed in light of the radiometric and spatial characteristics. To satisfy two conditions simultaneously and set the final treetop marker for the subsequent segmentation, we intersect two sets of treetops for each object by testing the proximity of each treetop detected by the nonmaximum suppression method to that of the maximum-distance method. If a treetop identified by the gray-level method is also located within a 3×3 window of the surrounding distance-based treetop, it will be labeled as the final treetop. For example, in Figure 13.4, there are five treetops identified by the gray-level nonmaximum suppression method, four of which coincidentally fall into the window of the surrounding distance-based treetops. Thus, those four treetops were recognized as the final treetops and markers, while the fifth one was filtered out as a pseudo treetop.

13.3.4 Marker-Controlled Watershed Segmentation

With the treetop markers generated by satisfying both radiometric and spatial characteristics, we utilized the marker-controlled watershed segmentation method with the goal of obtaining the individual-based tree-crown boundaries in each object. Watershed

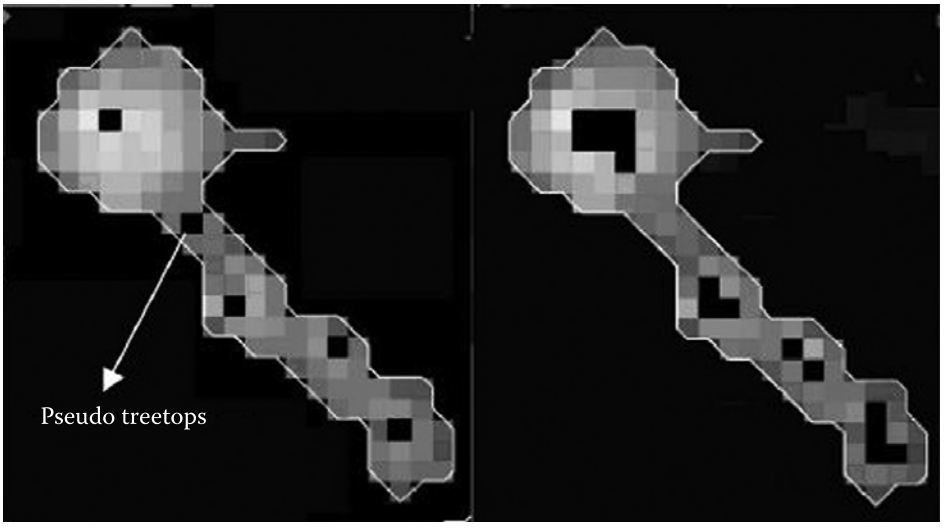

FIGURE 13.4
Treetops detection with both (a) radiometric—Markers from gray level—and (b) distance—Markers from geodesic distance—methods.

segmentation, as a nonlinear image processing method in mathematical morphology, was first introduced by Beucher and Lantuejoul and later defined mathematically by both Meyer and others (Pesaresi and Benediktsson 2001). The advantage of this method is to selectively preserve geometric or structural information while fulfilling the required tasks on the image. A further variant of this method is the so-called marker-controlled watershed segmentation, and it can be understood as follows. If we treat the gray-scale image as a topographic model, each pixel in the image will stand for the elevation at that point (Vincent and Soille 1991) and treetop markers will be the local maxima. By inverting the gray tone of the image, those markers will become the local minima lying in the valley. If water is introduced into this topographic model, each valley will collect water with the marker as the starting point, until the water runs over the watershed and infiltrates into the adjacent valley. Each watershed of the valley corresponds to one closed contour containing unique marker, and it can partition the whole area into different catchment basins. Consequently, those contours generated by the segmentation become the desired boundaries of individual tree crowns within the object.

One crucial factor for generating the desired contour is its correlation with the gray-level image patterns. In our study, we determine the tree-crown boundary by creating the geodesic skeleton with the use of the influence zones (Soille 2003). To begin with, the geodesic distance from each interior pixel to each treetop marker is calculated with the elementary disk SE. Next, the influence zone for a specified marker K_i is determined by counting the pixels whose geodesic distance to K_i is smaller than that to any other markers. Subsequently, the individual-based tree-crown boundary can be formed by delimiting the boundaries of those influence zones.

Compared to the traditional marker-controlled watershed segmentation method, our study has two apparent advantages. On the one hand, our segmentation task performs on the individual objects, as opposed to the entire image of the traditional segmentation method. In this way, we can eliminate the error that would otherwise be introduced by the background. On the other hand, the traditional marker-controlled watershed segmentation often leads to severe over-segmentation because of the presence of spurious local minima and maxima (Soille 2003); we tackled this problem by defining the marker first in view of the treetops' characteristics.

13.4 Results

To enhance the tree-crown boundaries, dyadic wavelet decomposition was implemented with the first three levels (2^1, 2^2, 2^3) considered. Accordingly, the gradient magnitude and direction were calculated in virtue of the wavelet coefficients obtained at each level. Edge probability could then be derived at the scale 2^1, 2^2, and 2^3 according to Equation 13.7, and the results are shown in Figure 13.5. By analyzing the evolution of image gradients over the scale space, we found that tree-crown boundaries were effectively strengthened, while the excessive textures that resulted from tree branches and twigs were largely suppressed. Moreover, the scale consistency was checked in terms of the harmonic mean, and the geometric consistency was conducted by using the gradient directions. With the updated edge probability achieved, the magnitude of the horizontal and vertical wavelet coefficients was adjusted and then an inverse wavelet transform was carried out.

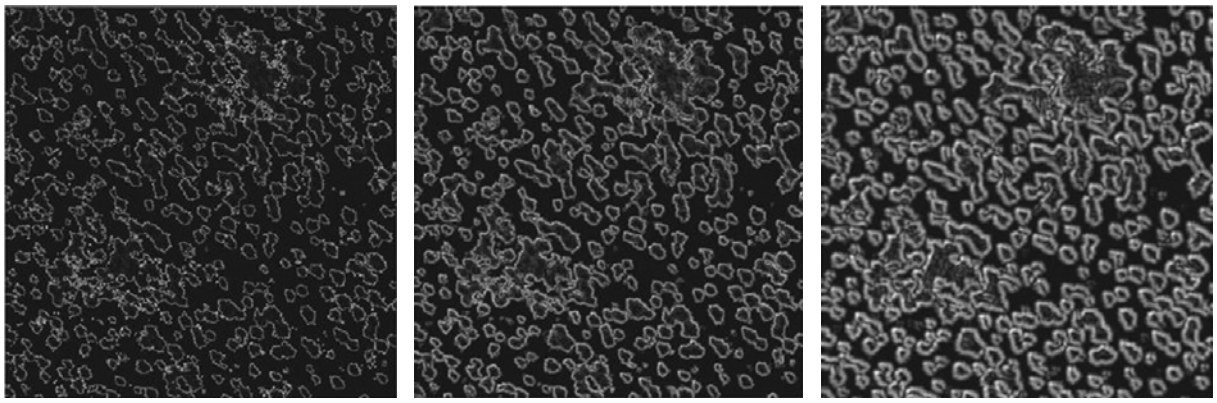

(a) (b) (c)

FIGURE 13.5
Edge probabilities at the scale 2^1 (a), 2^2 (b), and 2^3 (c).

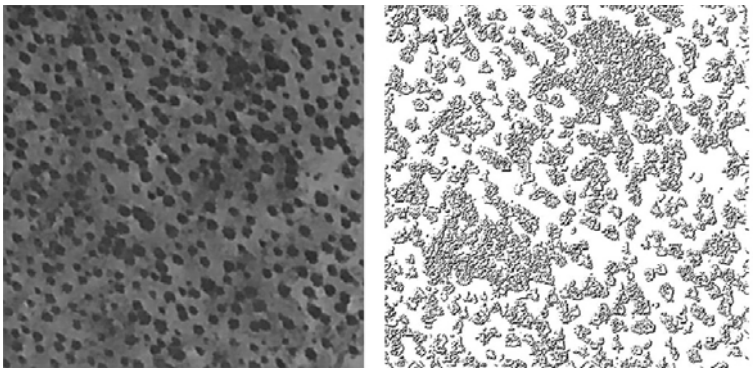

(a) (b)

FIGURE 13.6
Enhanced tree-crown boundaries from the multiscale wavelet decomposition (a) and the shaded relief of difference between the enhanced and original image (b).

After the edge-enhanced image was acquired (Figure 13.6), it was subtracted from the original image for illustrating the effect of the wavelet decomposition method. A shaded relief image denoting the difference between two images is presented in Figure 13.6. With a significant number of small textures within the tree crowns standing out in the difference image, our method can be proved efficient in strengthening the tree-crown boundaries, as well as in suppressing the textures inside. The enhanced image greatly alleviates the difficulty in the subsequent treetop detection and tree-crown delineation.

With the enhanced version of the image, we applied a two-stage approach, an edge-detection method followed by the marker-controlled watershed segmentation, and the final delineated tree crowns are shown in Figure 13.7. To evaluate our result, a total of 58 trees were selected and measured from the ground; 56 trees were correctly identified from the automated tree-crown delineation method, while the other two were undetected. For those 56 correctly identified trees, we first extracted the crown area from the image and then converted it to the radius based on a circular crown shape assumption. Subsequently, the radius derived from the image and that measured in the field were compared and regressed (Figure 13.8). The slope value in the regression model is 0.875, signifying that the crown size was underestimated from the automated method. The reason can be attributed to the fact that pixels on the tree-crown boundaries were not

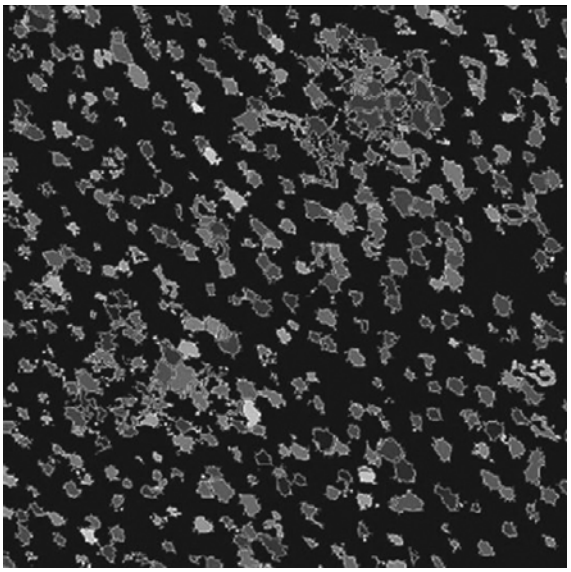

FIGURE 13.7
Final delineated tree crowns from the marker-controlled watershed segmentation method.

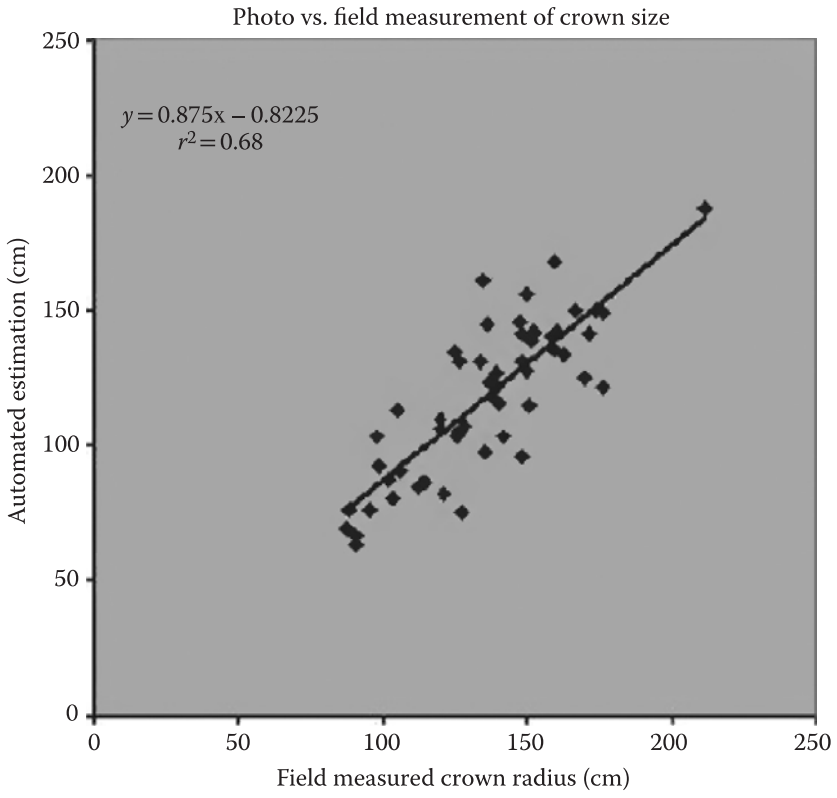

FIGURE 13.8
Regression of the tree-crown radius measured on the ground and that from the image based on 56 identified trees.

obviously detectable and may not be well recorded in the image. The R^2 in this case is 0.68, and it indicates that 68% variance of the automatically delineated tree-crown size can be explained by the regression model. The unexplained variance can actually be caused by the noise introduced when a circular shape was used to convert the irregular crown area to the radius value.

13.5 Discussion

With the developed multiscale scheme, promising tree-crown delineation was achieved. Out of 58 field-surveyed trees, 56 were identified in the image with the automated method. A comparison of crown size for 56 trees with R^2 value of 0.68 indicates the feasibility of delineating the tree crown from remote sensing imagery. Hence, it is necessary to perform an effective enhancement before the tree-crown boundary was delineated.

Traditionally, treetop extraction and tree-crown delineation are treated as separate procedures by most researchers. However, the solution of one part can usually assist in deriving the solution of the other. Owing to their close relationship, the integration of two parts tends to produce a more accurate result. In our algorithm, we filtered out spurious local minima and maxima by locating the treetops and then utilized those treetops as markers for delineating the tree-crown boundaries. The combination of two parts helps avoid the problem of over-segmentation to a great extent. Therefore, the derivation of treetop is indispensable and essential for determining the success of the individual tree-crown delineation.

With respect to the treetop detection, we utilize two methods by considering both radiometric and geometric characteristics. Our results have shown that the morphological information plays a crucial role in detecting the pseudo treetops generated by the radiometric nonmaximum suppression methods. However, existing algorithms have not effectively exploited such shape information. By superimposing a geometric restriction on the traditional gray-level method, we actually reduced the errors to a large degree.

By using treetops as the markers for delineating the individual tree-crown boundaries, we have effectively overcome the shortage of the traditional watershed segmentation method and generated a more accurate boundary image. Although our algorithm takes advantage of both spectral and spatial information for locating treetops and separating individual trees, there are still some potential problems deserving further research. One problem is the limitation of the assumptions. The spatially morphological algorithm for locating the treetops can be implemented only with the assumption that treetops are located around the vicinity of the center of a crown. However, it can only be satisfied within 15° of the nadir, and it may not be applicable to the trees outside of this range. To build a more robust algorithm, different treetop models based on the location of trees can be incorporated. Another problem is the inflexibility of the algorithm. In our methods, the σ value in the LOG edge detection, the window size of the nonmaximum suppression, the window size of the treetop intersection method, and the SE were all assigned a fixed value by virtue of the minimum tree-crown size. However, those parameters could be varied. Different scenarios should be evaluated to produce a more accurate result. Finally, tree-crown boundaries are sometimes inconsistent with gray-scale boundaries. The problem does not affect the trees viewed from the near-nadir direction, but may haunt those from outside the near-nadir range. For those regions, the silhouettes detected from edge-detection methods are sometimes inconsistent with the real tree-crown boundaries, which may be solved by using a 3D-based model.

13.6 Conclusion

In summary, tree-crown boundaries can be effectively enhanced and the internal texture can be largely suppressed by applying the multiscale wavelet decomposition method. The scale and geometric consistency check are critically important in the process of

enhancement by accounting for the tree's radiometric and morphological characteristics. Treetops can be more accurately detected by exploring the radiometric and spatial characteristics simultaneously. However, the spatial information is rarely utilized for locating the treetops because of the difficulty of expressing shape information in discrete image space. With the aid of mathematical morphology, we developed an approach to integrate the spatial information with the traditional radiometric method, which filtered out the pseudo treetops to a great extent. Tree crowns and treetops are closely related parameters, and the integration of two parts tends to produce a more accurate delineation result. By locating treetops with their special characteristics and using them as the markers for generating tree-crown contour, the marker-controlled watershed segmentation method sets a good example for combining treetop detection and tree-crown delineation under a unified framework. The result of marker-controlled watershed segmentation achieves a promising agreement with that from the field survey, indicating the feasibility of obtaining the tree-crown area from remote sensing imagery. In future work, a more robust tree-crown algorithm should be developed and tested in a range of forests, especially the undisturbed forest that has not been thinned.

References

Blazquez, C. 1989. "Computer-Based Image Analysis and Tree Counting with Aerial Color Infrared Photography." *Journal of Imaging Technology* 15:163–68.

Brandtberg, T. 1999. "Remote Sensing for Forestry Applications—A Historical Retrospect." CVonline: On-Line Compendium of Computer Vision [Online]. Accessed on August 6, 2012: http://www.dai.ed.ac.uk/CVonline/LOCAL_COPIES/BRANDTBERG/UK.html

Brandtberg, T., and F. Walter. 1998. "Automated Delineation of Individual Tree Crowns in High Spatial Resolution Aerial Images by Multiple-Scale Analysis." *Machine Vision and Applications* 11:64–73.

Clark, J. J. 1989. "Authenticating Edges Produced by Zero-Crossing Algorithms." *Pattern Analysis and Machine Intelligence, IEEE Transactions on* 11:43–57.

Dralle, K., and M. Rudemo. 1996. "Stem Number Estimation by Kernel Smoothing of Aerial Photos." *Canadian Journal of Forest Research* 26:1228–36.

Gong, P., G. S. Biging, S. Lee, X. Mei, Y. Sheng, R. Pu, B. Xu, K. P. Schwarzr, and M. Mostafa. 1999. "Photo Ecometrics for Forest Inventory." *Geographic Information Sciences* 5:9–14.

Gong, P., Y. Sheng, and G. Biging. 2002. "3D Model-Based Tree Measurement from High-Resolution Aerial Imagery." *Photogrammetric Engineering and Remote Sensing* 68:1203–12.

Gougeon, F. A. 1995. "A Crown-Following Approach to the Automatic Delineation of Individual Tree Crowns in High Spatial Resolution Aerial Images." *Canadian Journal of Remote Sensing* 21:274–84.

Lindeberg, T. 1993. "Detecting Salient Blob-Like Image Structures and Their Scales with a Scale-Space Primal Sketch: A Method for Focus-of-Attention." *International Journal of Computer Vision* 11:283–318.

Lindenmayer, D. B., and J. F. Franklin. 2002. *Conserving Forest Biodiversity: A Comprehensive Multi-Scaled Approach*. Washington, DC: Island Press.

Lu, Y., and R. C. Jain. 1992. "Reasoning About Edges in Scale Space." *Pattern Analysis and Machine Intelligence, IEEE Transactions on* 14:450–68.

Mallat, S. G. 1989. "A Theory for Multiresolution Signal Decomposition: The Wavelet Representation." *Pattern Analysis and Machine Intelligence, IEEE Transactions on* 11:674–93.

Marr, D., and E. Hildreth. 1980. "Theory of Edge Detection." *Proceedings of the Royal Society of London. Series B. Biological Sciences* 207:187–217.

Palace, M., M. Keller, G. P. Asner, S. Hagen, and B. Braswell. 2007. "Amazon Forest Structure from IKONOS Satellite Data and the Automated Characterization of Forest Canopy Properties." *Biotropica* 40:141–50.

Pesaresi, M., and J. A. Benediktsson. 2001. "A New Approach for the Morphological Segmentation of High-Resolution Satellite Imagery." *Geoscience and Remote Sensing, IEEE Transactions on* 39:309–20.

Pinz, A., M. B. Zaremba, H. Bischof, F. A. Gougeon, and M. Locas. 1993. "Neuromorphic Methods for Recognition of Compact Image Objects." *Machine Graphics and Vision* 2:209–29.

Pollock, R. 1996. *The Automatic Recognition of Individual Trees in Aerial Images of Forests Based on a Synthetic Tree Crown Image Model*. Department of Computer Science, Vancouver, Canada: University of British Columbia.

Scharcanski, J., C. R. Jung, and R. T. Clarke. 2002. "Adaptive Image Denoising Using Scale and Space Consistency." *Image Processing, IEEE Transactions on* 11:1092–101.

Sheng, Y., P. Gong, and G. Biging. 2001. "Model-Based Conifer-Crown Surface Reconstruction from High-Resolution Aerial Images." *PE & RS Photogrammetric Engineering and Remote Sensing* 67:957–65.

Soille, P. 2003. *Morphological Image Analysis: Principles and Applications.* New York: Springer-Verlag.

Spurr, S. H. 1948. *Aerial Photographs in Forestry*. New York: Ronald Press Company.

Tarp-Johansen, M. J. 2002. "Automatic Stem Mapping in Three Dimensions by Template Matching from Aerial Photographs." *Scandinavian Journal of Forest Research* 17:359–68.

Vincent, L., and P. Soille. 1991. "Watersheds in Digital Spaces: An Efficient Algorithm Based on Immersion Simulations." *IEEE Transactions on Pattern Analysis and Machine Intelligence* 13:583–98.

Wang, L. 2010. "A Multi-Scale Approach for Delineating Individual Tree Crowns with Very High Resolution Imagery." *Photogrammetric Engineering and Remote Sensing* 76:371–78.

Wang, L., P. Gong, and G. S. Biging. 2004. "Individual Tree-Crown Delineation and Treetop Detection in High-Spatial-Resolution Aerial Imagery." *Photogrammetric Engineering and Remote Sensing* 70:351–58.

Taylor and Francis, Hoboken, ISBN: 9781466556935